

# Commensurate-incommensurate transition in frustrated Wigner crystals

Raphaël Menu,<sup>1</sup> Jorge Yago Malo,<sup>2</sup> Vladan Vuletić,<sup>3</sup> Maria Luisa Chiofalo,<sup>2</sup> and Giovanna Morigi<sup>1</sup>

<sup>1</sup> *Theoretische Physik, Universität des Saarlandes, D-66123 Saarbrücken, Germany*

<sup>2</sup> *Dipartimento di Fisica Enrico Fermi, Università di Pisa and INFN, Largo B. Pontecorvo 3, I-56127 Pisa, Italy.*

<sup>3</sup> *Department of Physics, MIT-Harvard Center for Ultracold Atoms, and Research Laboratory of Electronics, Massachusetts Institute of Technology, Cambridge, Massachusetts 02139, USA.*

(Dated: November 27, 2023)

Geometric frustration in systems with long-range interactions is a largely unexplored phenomenon. In this work we analyse the ground state emerging from the competition between a periodic potential and a Wigner crystal in one dimension, consisting of a selforganized chain of particles with the same charge. This system is a paradigmatic realization of the Frenkel-Kontorova model with Coulomb interactions. We derive the action of a Coulomb soliton in the continuum limit and demonstrate the mapping to a massive (1+1) Thirring model with long-range interactions. Here, the solitons are *charged* fermionic excitations over an effective Dirac sea. The mismatch between the periodicities of potential and chain, giving rise to frustration, is a chemical potential whose amplitude is majorly determined by the Coulomb self-energy. The mean-field limit is a long-range antiferromagnetic spin chain with uniform magnetic field and predicts that the commensurate, periodic structures form a complete devil's staircase as a function of the charge density. Each step of the staircase correspond to the interval of stability of a stable commensurate phase and scales with the number  $N$  of charges as  $1/\ln N$ . This implies that there is no commensurate-incommensurate phase transition in the thermodynamic limit. For finite systems, however, the ground state has a fractal structure that could be measured in experiments with laser-cooled ions in traps.

*Introduction.* Geometric frustration describes the impossibility for a system to simultaneously minimize all competing interactions due to its geometry [1]. It is at the basis of fascinating phenomena in many-body physics, such as spin liquids and ice in antiferromagnets [2]. Moreover, it is at the origin of the paradigmatic commensurate-incommensurate phase transition [3–5]. This phase transition, that is at the center of this study, separates a so-called commensurate phase, where the ground state exhibits long-range order, from an incommensurate one, where the formation of defects is energetically favorable. This paradigm encompasses phenomena encountered in material science and condensed matter [3], including the growth a crystal on a substrate [6], domain walls in magnetically ordered structures [7], charge-density-wave order in high-temperature superconductors [8], and vortex pinning in superconductors [9].

In one dimension, the classical commensurate-incommensurate transition is captured by the minimal model introduced by Frenkel and Kontorova [4, 10]. This model describes the dynamics resulting from the interplay between a periodic one-dimensional potential, representing an underlying substrate that tends to pin particles, and the elastic forces between the particles, describing the harmonic vibrations of an ordered array. For nearest-neighbour interactions, the mismatch between the substrate periodicity and the array's characteristic length gives rise to dislocations (kinks), see Fig. 1(a). The ground state is a non-analytic function of the mismatch, taking the form of a complete devil's staircase [3]. The transition to the incommensurate structure is discontinuous and occurs when the energy to create a kink (topological soliton) vanishes, leading to kinks proliferation [3, 5, 11]. In the continuum limit the kink

is the solution of a sine-Gordon equation [5, 12, 13]. The quantized form of the sine-Gordon equation can be mapped to the action of a (1+1) massive Thirring model [14, 15], thereby connecting dislocations in a lattice with fermionic excitations over a Dirac vacuum. Experimentally, the FK model can be realised with laser-cooled, self-organized arrays of interacting atoms, where the substrate is an external periodic potential such as an optical lattice [16, 17] (see [18, 19] for implementations of deformable substrates). For interparticle potentials scaling as  $1/r^\alpha$  with the distance  $r$  and  $\alpha > 1$ , the dynamics is captured by the Tomonaga-Luttinger theory [20–22]:

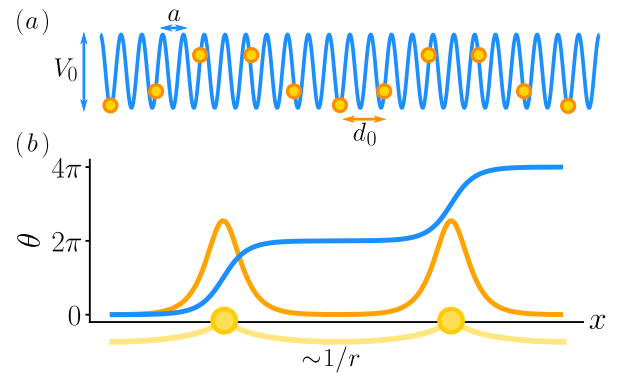


FIG. 1. (a) Schematic representation of the Wigner crystal confined by an optical lattice. The substrate potential leads to dislocation of the ions from the crystal's equilibrium position. (b) The dislocations (solitons) are displayed as phase shift  $\theta(x)$  along the chain axis  $x$  (blue). The first-order derivative of  $\theta(x)$  (orange) displays local maxima where the solitons are located. The yellow drawing illustrates that the solitons behave as interacting charges.

Dislocations are density waves and the commensurate-incommensurate transition is recovered in the properties of algebraically decaying correlation functions [22]. The FK model with Coulomb interactions,  $\alpha = 1$ , is peculiar: the decay of the correlations with the distance is slower than a power law, and any finite chain is a one-dimensional Wigner crystal [23]. This is a consequence of the non-additivity of the Coulomb energy in one dimension [24]. A further consequence is the anomalous dependence of the soliton's width (mass) on the chain size [25], which contrasts with the finite, size-independent mass for power-law interactions with  $\alpha > 1$ . Frustrated Wigner crystals are naturally realised with ion chains in traps [16, 17, 26–28]. Experiments with dozens of ions [19, 29, 30] identified features of the Aubry transition, namely, the transition from sliding to pinning controlled by the coupling strength with the substrate [4]. In these setups the soliton dynamics can be revealed with imaging and spectroscopic techniques [19, 31, 32], permitting to study their properties in the commensurate and in the incommensurate phase [33]. The experimental level of control can access quantum effects in the kinks dynamics [33–39]. This state-of-the-art brings forward the need to characterize the dynamics of solitons and the quantum phases of frustrated Wigner crystals, thereby shedding light onto the interplay between frustrations, long-range interactions, and quantum fluctuations.

*The action.* We consider  $N$  charged particles of mass  $m$  and confined along a chain of length  $L$ . For periodic boundary conditions the Coulomb repulsion is minimized by an ordered structure of periodicity  $d_0 = L/N$ . The charges perform long-range, harmonic vibrations about the equilibrium positions  $x_j^{(0)} = jd_0$ , the Hamiltonian reads [23, 40]

$$H_{\text{Wigner}} = \sum_j \frac{p_j^2}{2m} + \frac{K}{2} \sum_j \sum_{r>0} \frac{(x_{j+r} - x_j - rd_0)^2}{r^3},$$

with  $p_j$  and  $x_j$  canonically conjugated variables and  $K$  the stiffness. Frustration is introduced by a sinusoidal potential of depth  $V_0$  and periodicity  $a$ , see Fig. 1(a), such that for  $d_0 \gg a$  the new Hamiltonian reads  $H_{\text{FK}} = H_{\text{Wigner}} - \sum_j V_0 \cos(2\pi x_j/a)$  and the equations of motion describe a set of coupled pendula. It is convenient to introduce the static particle displacement  $u_j$  of the new chain equilibrium positions  $\bar{x}_j^{(0)}$  from the periodic ordering of a Wigner crystal  $jd_0$ ,  $u_j = \bar{x}_j^{(0)} - jd_0$ . A discommensuration, for which  $u_j \neq 0$ , breaks the translational symmetry and is represented by a finite value of the mismatch  $\delta = (d_0 - n_0 a)/a$ , with  $0 < \delta < 1$ . A dislocation is captured by the behavior of the phase  $\theta_j = \frac{2\pi}{a}(u_j + ja\delta)$  as a function of  $j$ , see Fig. 1(b). In the continuum limit  $\theta_j(t) \rightarrow \theta(x, t)$ , where  $x$  is the dimensionless position along the chain in units of the mean interparticle spacing  $d_0$ . The dynamics of the field  $\theta(x, t)$  is

governed by a modified sine-Gordon equation [25, 41, 42]

$$\frac{1}{v_s^2} \partial_t^2 \theta = \partial_x^2 \theta - M^2 \sin \theta + \frac{1}{3} \partial_x \int_1^{N/2} \frac{\partial_x \theta(x+u) + \partial_x \theta(x-u)}{u} du, \quad (1)$$

where the integral term accounts for the long-range Coulomb repulsion (see Supplemental Material (SM) A [43]). The equation is parametrized by a velocity  $v_s = \sqrt{3K/(2m)}$  and by a mass term  $M = \sqrt{8\pi^2 V_0/(3Kd^2)}$ , the solutions shall satisfy the constraint given by the mismatch  $\delta$ . For nearest-neighbor interactions the integral term vanishes:  $v_s$  is then the sound velocity and  $M$  the soliton mass. The kink's length is determined by  $1/M$  and the continuum limit requires  $1/M \gg 1$ . The integral term still preserves the soliton-like behavior and gives rise to an effective length that scales as  $\sqrt{\ln N}$  [25, 44] and tails that decay as  $1/r$  [25, 41, 42].

We here keep the integral term of Eq. (1) and observe that Eq. (1) is the Euler-Lagrange equation of the action  $\mathcal{S}$  (see SM A [43]):

$$\mathcal{S}[\theta] = \frac{1}{\beta^2} \int d\tau dx \left[ \frac{1}{2} (\partial_\tau \theta)^2 - \frac{1}{2} (\partial_x \theta - 2\pi\delta)^2 + M^2 \cos \theta - \frac{1}{6} \int_1^{N/2} \frac{du}{u} (\partial_x \theta(x) - 2\pi\delta) (\partial_x \theta(x+u) + \partial_x \theta(x-u) - 4\pi\delta) \right], \quad (2)$$

where  $\tau = v_s t$  is the rescaled time and  $\beta^2 = (\frac{2\pi}{a})^2 \sqrt{\frac{2\hbar^2}{3mK}}$  is an effective Planck constant, corresponding to the ratio between kinetic and Coulomb characteristic energy [45, 46]. The dynamics is now fully determined by the soliton mass  $M$ , the effective Planck constant  $\beta^2$ , and the mismatch  $\delta$ . The quantum field  $\theta(x, \tau)$  and its conjugate  $\partial_\tau \theta(x, \tau)$  satisfy the equal-time commutator  $[\theta(x, \tau), \partial_\tau \theta(x', \tau)] = i\beta^2 \delta(x - x')$ . The action in Eq. (2) extends to long-range interactions the action of the sine-Gordon model by an additional integral term, representing soliton-soliton interactions with Coulomb decay.

*Mapping to a long-range Thirring model.* Consider the spinor field  $\psi^\dagger = (\psi_1^\dagger, \psi_2^\dagger)$  with components [15]

$$\psi_j(x) = \frac{i^{(j-1)}}{\sqrt{2\pi}} \exp \left( -\frac{2\pi i}{\beta} \int_{-\infty}^x \partial_\tau \theta(u) du + (-1)^j \frac{i\beta}{2} \theta(x) \right). \quad (3)$$

Each fermion field ( $j = 1, 2$ ) corresponds to a different chirality. We linearize  $\psi_j(x)$  for slowly-varying soliton fields ( $|\partial_\tau \theta|, |\partial_x \theta| \ll 1$ ). Extending the procedure of Ref. [15] (see also SM A [43]) the action is brought to the Hamiltonian form  $H = \int dx (\mathcal{H}(x) - h' \rho(x))$ , where  $\rho(x) = \psi^\dagger \psi$  is the density of the fermion field. The chemical potential  $h'$  is proportional to the discommensuration:

$$h' = \delta \left( \frac{2\pi}{\beta} \right)^2 \left( 1 - \frac{2 \ln 2}{3} + \frac{2}{3} \ln N \right), \quad (4)$$

and the scaling with  $\ln N$  is due to a Coulomb selfenergy. The Hamiltonian density  $\mathcal{H}(x)$  is the (1+1) Thirring model for charged massive fermions:

$$\mathcal{H}(x) = -ic\bar{\psi}\gamma^1\partial_x\psi + \frac{g}{4}(\bar{\psi}\gamma^\mu\psi)(\bar{\psi}\gamma_\mu\psi) + M_0\bar{\psi}\psi + \frac{(2\pi)^2}{6\beta^2} \int_1^{N/2} \frac{du}{u} \rho(x) (\rho(x+u) + \rho(x-u)), \quad (5)$$

with the adjoint spin  $\bar{\psi} \equiv \psi^\dagger\gamma^0$  and  $\mu = 0, 1$  such that  $\gamma^0 = \sigma^z$ ,  $\gamma^1 = i\sigma^y$ . The dimensionless variables are the mass  $M_0 = \frac{\pi M^2}{\beta^2}$  and the speed  $c = \frac{2\pi}{\beta^2} + \frac{\beta^2}{8\pi}$ . The fermions display both contact interactions, with strength  $g = (\frac{2\pi}{\beta})^2 - (\frac{\beta}{2})^2$ , as well as long-range density-density interactions.

The mapping to the long-range Thirring Hamiltonian establishes an explicit link between frustration in an ion chain and a long-range lattice field theory. Now, the commensurate structure is gapped, with the filled Dirac sea of all negative-energy states, see Fig. 2, and the chemical potential set below the gap,  $h' < M_0$ . The topological defects are charged fermionic excitations at positive energy, their energy cost is the rescaled soliton mass  $M_0$ . For  $h' > M_0$  the energy for creating a soliton vanishes and the phase is incommensurate. The nature of the transition is not known. It is not possible, for instance, to draw an analogy with the nearest-neighbor case, where the Thirring model undergoes a Berezinskii-Kosterlitz-Thouless transition (BKT) as a function of  $M_0$  and fixed  $h'$  [47]. In fact, in the long-range case the scaling of the mismatch with the system size,  $h' \sim \ln N$ , indicates that the Coulomb interactions dominate, questioning whether a BKT may persist (see also [48, 49]).

*XXZ model and thermodynamic limit.* In order to understand the implications on the commensurate-incommensurate transition, we extend the procedure of Ref. [47, 50] to the long-range model. The continuous fermionic field becomes a single discrete field with discrete steps  $n$  over the grid  $d_0$  with the prescription  $\psi_1(n) \equiv \hat{f}_{2n}$  and  $\psi_2(n) \equiv \hat{f}_{2n+1}$ . In this picture, the Thirring Hamiltonian  $H$  is mapped to a model of interacting fermions on a lattice with a site-dependent chemical potential. We then apply the Jordan-Wigner transformation:  $\hat{\sigma}_n^- = \exp\left[-i\pi \sum_{k < n} \hat{f}_k^\dagger \hat{f}_k\right] \hat{f}_n$ ;  $\hat{\sigma}_n^+ = \hat{f}_n^\dagger \exp\left[i\pi \sum_{k < n} \hat{f}_k^\dagger \hat{f}_k\right]$  and  $\hat{\sigma}_n^z = \hat{f}_n^\dagger \hat{f}_n$ , and bring the model to a XXZ Hamiltonian of spin- $\frac{1}{2}$  particles in an external field (see SM B [43]):

$$\hat{H}_{\text{AFM}} = -\frac{c}{2} \sum_n (\hat{\sigma}_n^+ \hat{\sigma}_{n+1}^- + \hat{\sigma}_n^- \hat{\sigma}_{n+1}^+) + \frac{g}{2} \sum_n \hat{\sigma}_n^z \hat{\sigma}_{n+1}^z + \sum_n ((-1)^n M_0 - h') \hat{\sigma}_n^z + \frac{2\pi^2}{3\beta^2} \sum_n \sum_{|r| > 1} \frac{1}{|r|} \hat{\sigma}_n^z \hat{\sigma}_{n+r}^z. \quad (6)$$

The first line of  $\hat{H}_{\text{AFM}}$  is a nearest-neighbor XXZ model, the second line contains a magnetic field along  $z$  with

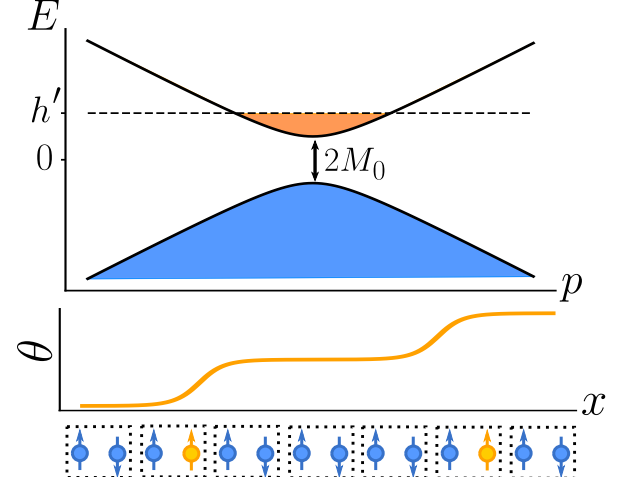


FIG. 2. Soliton-charged fermions correspondence. (upper panel) In the Thirring model the solitons are positive-energy excitation over a filled Dirac sea, where the gap is the soliton mass. The phase is commensurate when the chemical potential  $h'$  (controlled by the mismatch) falls within the gap. For  $h' > M_0$ , the solitons proliferate and the phase is incommensurate. The scaling of the chemical potential with the system size,  $h' \propto \ln N$ , suggest that the spectrum is effectively gapless in the thermodynamic limit. (lower panel) Interpretation of the spin-fermion equivalence in the discretized Thirring model, corresponding to a XXZ antiferromagnetic spin chain: Solitons are defects (in orange) in the staggered ordering of a spin chain.

a staggered component with amplitude  $M_0$  and a uniform term controlled by  $h'$ , and thus the mismatch. The last term is a long-range Ising term. Hamiltonian (6) describes the full extent of the quantum behaviour of a Wigner crystal in contact with a substrate. It encompasses the commensurate-incommensurate transition heralding the reorganization of the charged particles to fit the substrate's periodicity, with control field  $h'$ . In turn, the amplitude  $M_0$  of the staggered field controls the Aubry transition signaling the pinning of the crystal to its substrate. Now, for  $h' = 0$  the substrate imposes staggered order of the spins and the phase is an antiferromagnet. The homogeneous magnetic field  $h'$  (the mismatch) tends to flip spins in the up-oriented direction, therefore introducing defects (solitons) in the spin chain, as illustrated in the lower panel of Fig. 2.

The scaling of the terms in Eq. (6) with  $N$  is crucial. In fact, in one dimension the Coulomb interactions scales as  $N \ln N$ . We apply the prescription  $K \rightarrow K_N = K/\ln N$ , such that  $K_N$  remains finite in the thermodynamic limit [44]. This prescription is reminiscent of Kac's scaling, which restores the energy extensivity of long-range systems [24]. As a consequence,  $\beta^2$  shall be replaced by  $\beta^2 \sqrt{\ln N}$  in Eq. (6). Performing an expansion of the coefficients  $c$  and  $g$  at leading order in  $1/\ln N$ , we obtain that the short-range XXZ is proportional to  $\beta^2$ , while all other terms scale as  $1/\beta^2$  (See SM C [43]). Thus, for

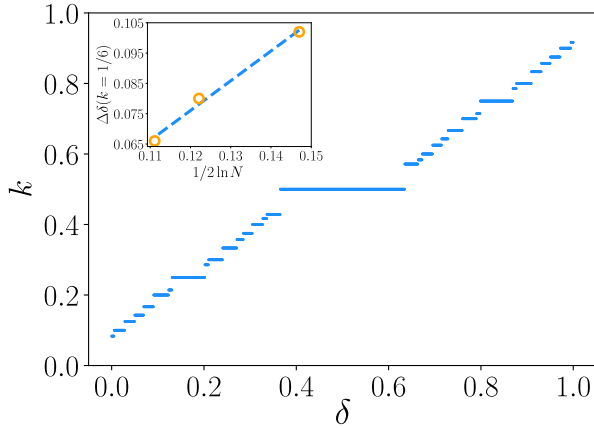


FIG. 3. Devil's staircase at finite  $N$ . Here, the fraction  $k$  of up-oriented spins is displayed as a function of the mismatch  $\delta$ . The size of the staircase steps depend on the system size. Inset: width of the plateau for the fraction  $k = 1/6$  as a function of  $\ln N$ : the plateau decreases with  $1/\ln N$ . The fraction is computed using the method of Ref. [52] for a chain of  $N = 100$  ions ( $N_s = 200$  spins) and for  $\tilde{M}/J_0 = 0.1$ .

$\beta^2 \gg 1$  the ground state is the one of the short range XXZ Hamiltonian. In the following we discuss the opposite case,  $\beta^2 \ll 1$ , characterizing trapped-ion systems [46, 51].

*Devil's staircase.* At leading order in an expansion in  $\beta \ll 1$  the Hamiltonian is the mean-field energy (see SM C [43]):

$$E_{\text{mf}}[\{\sigma_j\}] = \frac{1}{2} \sum_{i,j} \frac{J_0}{|i-j|} \sigma_i \sigma_j - \sum_i \tilde{B}_i \sigma_i, \quad (7)$$

and is a function of the string  $\{\sigma_j\}$  with  $\sigma_j = 0, 1$ . The parameters of Eq. (7) are the interaction amplitude  $J_0 = \gamma/(2 \ln N)$  and the magnetic field  $\tilde{B}_i = \gamma(\delta - \tilde{M}(-1)^i)$ , with  $\gamma = 8\pi^2/(3\beta^2)$  a scaling factor. Field  $\tilde{B}_i$  is the sum of the uniform magnetic field  $\delta$ , corresponding to the mismatch, and of the staggered magnetic field  $M = \pi V_0/(Ka^2)$ , corresponding to the soliton mass. At fixed mismatch and varying the potential depth,  $\tilde{B}_i$  controls the Aubry transition from sliding to pinned phase. Instead, at fixed potential depth  $V_0$ , the magnetic field controls the transition to an incommensurate structure. We analyse the latter following [53]. A commensurate configuration  $\{\sigma_j\}$  at  $\delta = 0$  is characterized by the number  $k = r/n$  of up-oriented spins (magnetization) with  $r, n \in \mathbb{N}$ . The transition to an incommensurate structure occurs for the values of  $\delta$  at which flipping a spin has zero cost, and occurs at the minimum  $\delta_{\min}(k)$  and maximum value  $\delta_{\max}(k)$  of the mismatch. In the interval  $(\delta_{\min}(k), \delta_{\max}(k))$  the configuration is gapped and the commensurate phase is stable. The width of this interval,  $\Delta\delta = \delta_{\max}(k) - \delta_{\min}(k)$ , is given by [53]

$$\Delta\delta \approx \frac{1}{\ln N} \sum_{p=1}^{+\infty} \frac{1}{p^2 n^2 - 1} \approx \frac{\zeta(2)}{n^2 \ln N}, \quad (8)$$

and determines the gap of the corresponding commensurate phase at temperature  $T = 0$ . At finite  $N$  the ground state is a complete Devil's staircase, as shown on Fig. 3. The inset illustrates how the plateau  $\Delta\delta$  decreases with  $N$  as  $\ln N$ . This behavior predicts that the devil's staircase disappears in the thermodynamic limit and is consistent with the result of [54], indicating that the fractal dimension of the ground state of Eq. (7) is  $D_F = 1$ . It is strikingly different from the case of power-law interactions  $1/r^\alpha$  with  $\alpha > 1$ , where  $D_F > 1$  and the devil's staircase is complete for  $N \rightarrow \infty$  [54]. Therefore, for Coulomb interactions there is no commensurate-incommensurate phase transition in the thermodynamic limit.

*Experimental realizations.* Given the slow convergence of  $1/\ln N$ , a commensurate-incommensurate transition shall be measurable in any finite chain. One assumption of our study is the equidistance of the ions forming the Wigner crystal. This is typically realized in the central region of linear Paul traps [55] or in ring traps [56] and requires several dozens of ions. A feasibility study for 5 ions in a linear Paul trap [37] shows that, although the dynamics is strongly affected by finite-size effects, the calculated phase diagram is qualitatively consistent with our predictions. The commensurate-incommensurate transition can be detected by measuring the low-frequency part of the vibrational spectrum [19, 30, 57]. Features of the devil's staircase are visible as long as thermal excitations are smaller than the gap [45, 58]. Using the parameters of Ref. [30], for a chain of 100 ions  $^{171}\text{Yb}^+$  with interparticle distance  $d_0 = 6\mu\text{m}$  and lattice periodicity  $a = 185\text{nm}$ , steps of the Devil's staircase with magnetization  $k = m/n$  will be measured for temperatures  $T \lesssim 1\text{ mK}/n$ . Quantum effects at the transition are scaled by the parameter  $\beta^2 \simeq 10^{-5}$  and could be visible in a narrow parameter region, see Ref. [33, 45] for some estimates.

*Conclusions.* The dynamics of solitons in Coulomb chains can be mapped to massive charged fermions, that are created over the Dirac sea of a Coulomb (1+1)-Thirring model. The mean-field model is a long-range antiferromagnetic spin chain in a uniform magnetic field. This model predicts that the commensurate-incommensurate transition becomes a crossover for Coulomb interactions, with the transition point moving to infinity in the thermodynamic limit. This result is consistent with the predictions on the critical behavior of other long-range models [48, 49, 59]. For any finite chain, however, a commensurate-incommensurate crossover can be observed. The corresponding commensurate configurations possess fractional excitations [53], thereby drawing an intriguing analogy between frustrated Wigner chain and the fractional quantum Hall effect in one dimension [60]. This shows the power of Wigner crystals of ions as natural quantum simulators of non-trivial lattice-gauge field theoretical and topological models. Future studies will characterize the quantum dynamics of finite chains at the transition.

*Acknowledgments* The authors acknowledge discussions with O. Chelpanova, S. B. Jäger, J. Koziol, H. Landa, J. Marino, T. Mehlstäubler, and S. Kelly. G.M. is grateful to B. Mattioli and S. Mellini for inspiring comments, and V. Ortolani for pointing out relevant references. This work was supported by the Deutsche Forschungsgemeinschaft (DFG, German Research Foundation), with the CRC-TRR 306 “QuCoLiMa”, Project-ID No. 429529648, by the German Ministry of Education and Research (BMBF) via the project NiQ (“Noise in Quantum Algorithm”), and in part by the National Science Foundation under Grants No. NSF PHY-1748958 and PHY-2309135. J.Y.M. was supported by the Euro-

pean Social Fund REACT EU through the Italian national program PON 2014-2020, DM MUR 1062/2021. M.L.C. acknowledges support from the MIT-UNIPI program and by the National Quantum Science and Technology Institute (NQSTI), spokes 2 and 10, funded under the National Recovery and Resilience Plan (NRRP), Mission 4 Component 2 Investment 1.3 - Call for tender No. 341 of 15/03/2022 of Italian Ministry of University and Research, funded by the European Union NextGenerationEU, award number PE0000023, Concession Decree No. 1564 of 11/10/2022 adopted by the Italian Ministry of University and Research, CUP D93C22000940001.

---

[1] R. Moessner and A. P. Ramirez, *Phys. Today* **59**, 24 (2006).

[2] L. Balents, *Nature* **464**, 199 (2010).

[3] P. Bak, *Reports on Progress in Physics* **45**, 587 (1982).

[4] O. Braun and Y. Kivshar, *The Frenkel-Kontorova Model: Concepts, Methods, and Applications* (Springer, New York, 2004).

[5] V. Pokrovskij and A. Talapov, *Theory of incommensurate crystals* (Harwood Academic Publishers, New York, 1984).

[6] C. R. Woods, L. Britnell, A. Eckmann, R. S. Ma, J. C. Lu, H. M. Guo, X. Lin, G. L. Yu, Y. Cao, R. V. Gorbatchev, A. V. Kretinin, J. Park, L. A. Ponomarenko, M. I. Katsnelson, Y. N. Gornostyrev, K. Watanabe, T. Taniguchi, C. Casiraghi, H.-J. Gao, A. K. Geim, and K. S. Novoselov, *Nature Physics* **10**, 451 (2014).

[7] K. Kuroda, Y. Arai, N. Rezaei, S. Kunisada, S. Sakuragi, M. Alaei, Y. Kinoshita, C. Bareille, R. Noguchi, M. Nakayama, S. Akebi, M. Sakano, K. Kawaguchi, M. Arita, S. Ideta, K. Tanaka, H. Kitazawa, K. Okazaki, M. Tokunaga, Y. Haga, S. Shin, H. S. Suzuki, R. Arita, and T. Kondo, *Nat Commun* **11**, 2888 (2020).

[8] X. Y. Feng, Z. Zhao, J. Luo, J. Yang, A. F. Fang, H. T. Yang, H. J. Gao, R. Zhou, and G.-q. Zheng, *npj Quantum Materials* **8**, 23 (2023).

[9] O. Daldini, P. Martinoli, J. L. Olsen, and G. Berner, *Phys. Rev. Lett.* **32**, 218 (1974).

[10] Y. Frenkel and T. Kontorova, *Zh. Eksp. Teor. Fiz.* **8**, 1340 (1938).

[11] H. P. Büchler, G. Blatter, and W. Zwerger, *Phys. Rev. Lett.* **90**, 130401 (2003).

[12] F. C. Frank, J. H. van der Merwe, and N. F. Mott, *Proceedings of the Royal Society of London. Series A. Mathematical and Physical Sciences* **198**, 205 (1949).

[13] J. Rubinstein, *Journal of Mathematical Physics* **11**, 258 (2003).

[14] S. Coleman, *Phys. Rev. D* **11**, 2088 (1975).

[15] S. Mandelstam, *Phys. Rev. D* **11**, 3026 (1975).

[16] T. Pruttivarasin, M. Ramm, I. Talukdar, A. Kreuter, and H. Häffner, *New Journal of Physics* **13**, 075012 (2011).

[17] M. Cetina, A. Bylinskii, L. Karpa, D. Gangloff, K. M. Beck, Y. Ge, M. Scholz, A. T. Grier, I. Chuang, and V. Vuletić, *New Journal of Physics* **15**, 053001 (2013).

[18] T. Fogarty, C. Cormick, H. Landa, V. M. Stojanović, E. Demler, and G. Morigi, *Phys. Rev. Lett.* **115**, 233602 (2015).

[19] J. Kiethe, R. Nigmatullin, D. Kalincev, T. Schmirander, and T. Mehlstäubler, *Nature Commun.* **8**, 15364 (2017).

[20] M. A. Cazalilla, R. Citro, T. Giamarchi, E. Orignac, and M. Rigol, *Rev. Mod. Phys.* **83**, 1405 (2011).

[21] V. Kasper, J. Marino, S. Ji, V. Gritsev, J. Schmiedmayer, and E. Demler, *Phys. Rev. B* **101**, 224102 (2020).

[22] M. Dalmonte, G. Pupillo, and P. Zoller, *Phys. Rev. Lett.* **105**, 140401 (2010).

[23] H. J. Schulz, *Phys. Rev. Lett.* **71**, 1864 (1993).

[24] A. Campa, T. Dauxois, and S. Ruffo, *Physics Reports* **480**, 57 (2009).

[25] H. Landa, C. Cormick, and G. Morigi, *Condensed Matter* **5** (2020), 10.3390/condmat5020035.

[26] García-Mata, I., Zhirov, O. V., and Shepelyansky, D. L., *Eur. Phys. J. D* **41**, 325 (2007).

[27] C. Cormick and G. Morigi, *Phys. Rev. A* **87**, 013829 (2013).

[28] A. Vanossi, N. Manini, M. Urbakh, S. Zapperi, and E. Tosatti, *Rev. Mod. Phys.* **85**, 529 (2013).

[29] R. B. Linnet, I. D. Leroux, M. Marciante, A. Dantan, and M. Drewsen, *Phys. Rev. Lett.* **109**, 233005 (2012).

[30] A. Bylinskii, D. Gangloff, I. Counts, and V. Vuletić, *Nature Materials* **15**, 717 (2016).

[31] J. Kiethe, R. Nigmatullin, T. Schmirander, D. Kalincev, and T. E. Mehlstäubler, *New Journal of Physics* **20**, 123017 (2018).

[32] J. Brox, P. Kiefer, M. Bujak, T. Schaetz, and H. Landa, *Phys. Rev. Lett.* **119**, 153602 (2017).

[33] D. A. Gangloff, A. Bylinskii, and V. Vuletić, *Phys. Rev. Research* **2**, 013380 (2020).

[34] T. Zanca, F. Pellegrini, G. E. Santoro, and E. Tosatti, *Proceedings of the National Academy of Sciences* **115**, 3547 (2018).

[35] F. R. Krajewski and M. H. Müser, *Phys. Rev. Lett.* **92**, 030601 (2004).

[36] F. R. Krajewski and M. H. Müser, *The Journal of chemical physics* **122** **12**, 124711 (2005).

[37] P. M. Bonetti, A. Rucci, M. L. Chiofalo, and V. Vuletić, *Phys. Rev. Res.* **3**, 013031 (2021).

[38] L. Timm, L. A. Rüffert, H. Weimer, L. Santos, and T. E. Mehlstäubler, *Phys. Rev. Res.* **3**, 043141 (2021).

[39] Chelpanova, Oksana, Kelly, Shane P., Morigi, Giovanna, Schmidt-Kaler, Ferdinand, and Marino, Jamir, *EPL*

143, 25002 (2023).

[40] S. Fishman, G. De Chiara, T. Calarco, and G. Morigi, *Phys. Rev. B* **77**, 064111 (2008).

[41] V. L. Pokrovsky and A. Virosztek, *Journal of Physics C: Solid State Physics* **16**, 4513 (1983).

[42] O. M. Braun, Y. S. Kivshar, and I. I. Zelenskaya, *Phys. Rev. B* **41**, 7118 (1990).

[43] See Supplemental Material [url] for (A) the full derivation of the (1+1) Thirring model with long-range interactions starting from the long-range Frenkel-Kontorova model, (B) the lattice field theoretical description of the Thirring model and its mapping onto a spin model, (C) the discussion of the Kac scaling of long-range interactions and the mean-field limit. The Supplementary Materials include the references [24, 44].

[44] G. Morigi and S. Fishman, *Phys. Rev. E* **70**, 066141 (2004).

[45] E. Shimshoni, G. Morigi, and S. Fishman, *Phys. Rev. Lett.* **106**, 010401 (2011).

[46] P. Silvi, G. De Chiara, T. Calarco, G. Morigi, and S. Montangero, *Annalen der Physik* **525**, 827 (2013).

[47] M. C. Bañuls, K. Cichy, Y.-J. Kao, C.-J. D. Lin, Y.-P. Lin, and D. T.-L. Tan, *Phys. Rev. D* **100**, 094504 (2019).

[48] G. Giachetti, N. Defenu, S. Ruffo, and A. Trombettoni, *Phys. Rev. Lett.* **127**, 156801 (2021).

[49] G. Giachetti, A. Trombettoni, S. Ruffo, and N. Defenu, *Phys. Rev. B* **106**, 014106 (2022).

[50] L. Susskind, *Phys. Rev. D* **16**, 3031 (1977).

[51] D. Podolsky, E. Shimshoni, P. Silvi, S. Montangero, T. Calarco, G. Morigi, and S. Fishman, *Phys. Rev. B* **89**, 214408 (2014).

[52] J. A. Koziol, A. Duft, G. Morigi, and K. P. Schmidt, *SciPost Phys.* **14**, 136 (2023).

[53] P. Bak and R. Bruinsma, *Phys. Rev. Lett.* **49**, 249 (1982).

[54] R. Bruinsma and P. Bak, *Phys. Rev. B* **27**, 5824 (1983).

[55] D. H. E. Dubin, *Phys. Rev. E* **55**, 4017 (1997).

[56] H.-K. Li, E. Urban, C. Noel, A. Chuang, Y. Xia, A. Ransford, B. Hemmerling, Y. Wang, T. Li, H. Häffner, and X. Zhang, *Phys. Rev. Lett.* **118**, 053001 (2017).

[57] A. Bylinskii, D. Gangloff, and V. Vuletić, *Science* **348**, 1115 (2015).

[58] J. Kiethe, L. Timm, H. Landa, D. Kalincev, G. Morigi, and T. E. Mehlstäubler, *Phys. Rev. B* **103**, 104106 (2021).

[59] M. F. Maghrebi, Z.-X. Gong, and A. V. Gorshkov, *Phys. Rev. Lett.* **119**, 023001 (2017).

[60] P. Rotondo, L. G. Molinari, P. Ratti, and M. Gherardi, *Phys. Rev. Lett.* **116**, 256803 (2016).

## Appendix A: Derivation of the (1+1)-Thirring model with long-range interactions

Considering  $N$  ions of mass  $m$  forming a Wigner crystal of stiffness  $K$ , the local phase shift  $\theta_j$  attached to the  $j$ -th ion follows the the classical equation of motion

$$m\ddot{\theta}_j - \sum_{r \neq 0} \frac{K}{|r|^3} (\theta_{j+r} - \theta_j - 2\pi\delta r) + \frac{(2\pi)^2 V_0}{a^2} \sin \theta = 0,$$

where  $\delta$  is the discommensuration. In the limit where the phase shifts  $\theta_j$  can be treated as one single field  $\theta(x, t)$

(where  $x$  is expressed in units of  $d_0$ ) whose equation of motion is the one given by Eq. (1):

$$\frac{1}{v_s^2} \partial_t^2 \theta = \partial_x^2 \theta - M^2 \sin \theta + \frac{1}{3} \partial_x \int_1^{N/2} \frac{\theta'(x+u) + \theta'(x-u)}{u} du,$$

$$\text{with } v_s = \sqrt{\frac{3K}{2m}} \text{ and } M = \frac{2\pi}{a} \sqrt{\frac{2V_0}{3K}}.$$

It is simple to verify that the long-range sine-Gordon model is the Euler-Lagrange equation of the Lagrange density  $\mathcal{L}$ , which gives the action  $\mathcal{S}$  of Eq. (2). Let us note that the discommensuration  $\delta$  introduce constraints on the solution of the Euler-Lagrange equation to be energetically favourable.

The mapping from the quantum sine-Gordon to the Thirring model is performed by fermionizing the bosonic field  $\theta(x, \tau)$  and its conjugate  $\dot{\theta}(x, \tau) = \partial_\tau \theta(x, \tau)$ . Two fermionic species with different chirality are introduced by the Mandelstam transformation:

$$\begin{aligned} \psi_1(x) &= \frac{1}{\sqrt{2\pi}} \exp \left( -\frac{2\pi i}{\beta} \int_{-\infty}^x \dot{\theta}(u) du - \frac{i\beta}{2} \theta(x) \right), \\ \psi_2(x) &= \frac{i}{\sqrt{2\pi}} \exp \left( -\frac{2\pi i}{\beta} \int_{-\infty}^x \dot{\theta}(u) du + \frac{i\beta}{2} \theta(x) \right). \end{aligned}$$

Assuming that the soliton field  $\theta(x, \tau)$  is slowly varying, then the Baker-Campbell-Hausdorff formula

$$e^A e^B = e^{A+B} e^{[A,B]/2},$$

in the case where the commutator  $[A, B]$  is a scalar quantity leads to the relation

$$\begin{aligned} \psi_1^\dagger(x+1) \psi_1(x) &= -\frac{i}{\sqrt{2\pi}} \exp \left[ \frac{2\pi i}{\beta} \dot{\theta}(x) + \frac{i\beta}{2} \theta'(x) \right] \\ &\simeq -\frac{i}{2\pi} + \left( \frac{1}{\beta} \dot{\theta}(x) + \frac{\beta}{4\pi} \theta'(x) \right). \end{aligned}$$

A renormalization of the total fermion number  $\psi^\dagger \psi = \psi_1^\dagger \psi_1 + \psi_2^\dagger \psi_2$ , eliminates the constant term in the previous expression. We use then the approximation  $\psi_j^\dagger(x+1) \psi_j(x) = \psi_j^\dagger(x) \psi_j(x)$ , to derive the relations

$$\begin{aligned} \frac{\beta}{2\pi} \theta'(x) &= \psi_1^\dagger(x) \psi_1(x) + \psi_2^\dagger(x) \psi_2(x) \\ \frac{2}{\beta} \dot{\theta}(x) &= \psi_1^\dagger(x) \psi_1(x) - \psi_2^\dagger(x) \psi_2(x) \\ \cos(\beta\theta(x)) &= -\pi(\psi_1^\dagger(x) \psi_2(x) + \psi_2^\dagger(x) \psi_1(x)). \end{aligned}$$

Additionally, the local density of fermions can be related to kinetic effects via the relations

$$\begin{aligned} i\psi_1^\dagger(x) \partial_x \psi_1(x) &= \pi(\psi_1^\dagger(x) \psi_1(x))^2 \\ -i\psi_2^\dagger(x) \partial_x \psi_2(x) &= \pi(\psi_2^\dagger(x) \psi_2(x))^2. \end{aligned}$$

As a result, following the substitution  $\theta \rightarrow \beta\theta$ , the long-range sine-Gordon Hamiltonian reading

$$H = \int dx \left[ \frac{1}{2} \dot{\theta}^2(x) + \frac{1}{2} \left( \theta'(x) - \frac{2\pi\delta}{\beta} \right)^2 - \frac{M^2}{\beta^2} \cos(\beta\theta(x)) \right. \\ \left. + \frac{1}{6} \int_1^{N/2} \frac{du}{u} (\theta'(x)) (\theta'(x+u) + \theta'(x-u)) \right] \\ - \frac{4\pi\delta}{3\beta} \ln\left(\frac{N}{2}\right) \int dx \theta'(x)$$

transforms into a fermionic Hamiltonian:

$$H = \int dx \left[ ic\psi^\dagger \sigma^z \partial_x \psi + g\psi_1^\dagger \psi_1 \psi_2^\dagger \psi_2 + M_0 \psi^\dagger \sigma^x \psi \right. \\ \left. + \frac{(2\pi)^2}{6\beta^2} \int_1^{N/2} \frac{du}{u} \rho(x) (\rho(x+u) + \rho(x-u)) \right] \\ - h' \int dx \rho(x).$$

The speed of light  $c$ , the contact interaction  $g$ , the fermion mass  $M_0$  and the chemical potential  $h'$  follow the definitions introduced in the main text.

This Hamiltonian describes the behaviour of the system in the Weyl representation of fermionic fields. We can cast the model in Dirac representation via the transformation  $\psi \rightarrow S\psi$ , where the matrix  $S$  reads

$$S = \frac{1}{\sqrt{2}} \begin{pmatrix} 1 & 1 \\ 1 & -1 \end{pmatrix}.$$

According to this prescription,  $S\sigma^x S = \sigma^z$  and  $S\sigma^z S = \sigma^x$ . The Hamiltonian can then be expressed as in Eq. (5), namely as  $H = H_0 - h' \int dx \rho(x)$ , where

$$H_0 = \int dx \left[ -ic\bar{\psi} \gamma^1 \partial_x \psi + \frac{g}{4} (\bar{\psi} \gamma^\mu \psi) (\bar{\psi} \gamma_\mu \psi) + M_0 \bar{\psi} \psi \right] \\ + \frac{(2\pi)^2}{6\beta^2} \int dx \int_1^{N/2} \frac{du}{u} \rho(x) (\rho(x+u) + \rho(x-u)).$$

The Dirac gamma matrices here read then  $\gamma^0 = \sigma^x$  and  $\gamma^1 = i\sigma^y$ .

## Appendix B: Discretization of the fields

The (1+1)-Thirring Hamiltonian is discretized following the prescription: we introduce a single discrete fermionic field whose value on even sites correspond to  $\psi_1$  and  $\psi_2$  on odd sites, hence  $\psi_1(x = n) \equiv \hat{f}_{2n}$  and  $\psi_2(x = n) \equiv \hat{f}_{2n+1}$ . Therefore, integrals transform into discrete sums as  $\int dx \rightarrow \sum_n$  and the Thirring model becomes

$$\hat{H} = -\frac{ic}{2} \sum_n (\hat{f}_{n+1}^\dagger \hat{f}_n - \hat{f}_n^\dagger \hat{f}_{n+1}) + \frac{g}{2} \sum_n \hat{f}_{n+1} \hat{f}_{n+1}^\dagger \hat{f}_n \hat{f}_n^\dagger \\ + \sum_n ((-1)^n - h') \hat{f}_n^\dagger \hat{f}_n + \frac{2\pi^2}{3\beta^2} \sum_n \sum_{|r|>1} \frac{1}{|r|} \hat{f}_n^\dagger \hat{f}_n \hat{f}_{n+r}^\dagger \hat{f}_{n+r}.$$

Discretized fermionic systems can be mapped onto spin models by the means of a Jordan-Wigner transformation that identifies the local number of fermions as the orientation of a spin- $\frac{1}{2}$ :  $|1\rangle \leftrightarrow | \uparrow \rangle$  and  $|0\rangle \leftrightarrow | \downarrow \rangle$ . As a result, one can deduce a simple relation between the fermionic and the spin operators:  $\hat{f}_n^\dagger \hat{f}_n = \hat{S}_n^z + \frac{1}{2} = \hat{\sigma}_n^z$ . And to reconcile both the fermionic and  $SU(2)$  spin algebra, the spin-fermion transformation yields  $\hat{\sigma}_n^- = \exp\left[-i\pi \sum_{k < n} \hat{f}_k^\dagger \hat{f}_k\right] \hat{f}_n$  and  $\hat{\sigma}_n^+ = \hat{f}_n^\dagger \exp\left[-i\pi \sum_{k < n} \hat{f}_k^\dagger \hat{f}_k\right]$ . The corresponding spin-Hamiltonian then takes the form of the XXZ model with site-dependent magnetic field and long-range Ising interactions of Eq. (6).

## Appendix C: Kac scaling and mean-field limit

In the following, we discuss the derivation of the mean-field model by means of the rescaling of the spring stiffness. In one dimension, the energy contribution of Coulomb interactions scales as  $N \ln N$ . We apply the so called Kac scaling  $K \rightarrow K_N = K/\ln N$ , such that  $K_N$  remains finite in the thermodynamic limit. Using this scaling in all expression  $\beta^2$  shall be replaced by  $\beta^2 \sqrt{\ln N}$  and consequently

$$c_N = \sqrt{\ln N} \frac{1}{\beta^2} \left( \frac{\beta^4}{8\pi} + \frac{2\pi}{\ln N} \right) \\ g_N = \sqrt{\ln N} \frac{1}{\beta^2} \left( -\frac{\beta^4}{4} + \frac{4\pi^2}{\ln N} \right)$$

At leading order in an expansion in  $1/\ln N$  then

$$c_N \sim \sqrt{\ln N} \frac{\beta^2}{8\pi} \\ g_N \sim -\sqrt{\ln N} \frac{\beta^2}{4}.$$

Moreover, using Kac's scaling the soliton mass acquires a scaling with  $\sqrt{\ln N}$  from the dependence on both the stiffness  $K$  as well as from  $\beta^2$ :

$$M_{0,N} = \sqrt{\ln N} \frac{8\pi^2}{3\beta^2} \frac{\pi V_0}{Ka^2}. \quad (\text{C1})$$

With this prescription, the scaling of the uniform magnetic field becomes:

$$h'_N \approx \sqrt{\ln N} \frac{8\pi^2}{3\beta^2} \delta, \quad (\text{C2})$$

Finally, the Coulomb interaction term is now multiplied by the factor  $2\pi^2/(3\beta^2 \sqrt{\ln N})$ . After collecting the common factor  $\sqrt{\ln N}/\beta^2$ , the XXZ Hamiltonian, Eq. (6),

takes the form

$$\begin{aligned}
\hat{H}_{\text{AFM}} = & -\frac{\beta^2}{8\pi} \sum_n (\hat{\sigma}_n^+ \hat{\sigma}_{n+1}^- + \hat{\sigma}_n^- \hat{\sigma}_{n+1}^+) \\
& - \frac{\beta^2}{8} \sum_n \hat{\sigma}_n^z \hat{\sigma}_{n+1}^z \\
& + \frac{8\pi^2}{3\beta^2} \sum_n \left( (-1)^n \frac{\pi V_0}{Ka^2} - \delta \right) \hat{\sigma}_n^z \\
& + \frac{2\pi^2}{3\beta^2 \ln N} \sum_n \sum_{|r|>1} \frac{1}{|r|} \hat{\sigma}_n^z \hat{\sigma}_{n+r}^z,
\end{aligned}$$

which is now extensive. With this rescaling, now for  $\beta^2 \gg 1$  the ground state is the one of the short range XXZ Hamiltonian while for  $\beta^2 \ll 1$  the Hamiltonian reduces to Eq. (7). Note that the limit  $N \rightarrow \infty$  does not commute with the expansion on  $\beta$ , a property characteristic of long-range interactions [24, 44].